

Birefringence of macromolecules

Wiener's theory revisited, with applications to DNA and tobacco mosaic virus

Rudolf Oldenbourg and Teresa Ruiz

Martin Fisher School of Physics, Brandeis University, Waltham, Massachusetts 02254

ABSTRACT We summarize Wiener's theory of the dielectric constant of heterogeneous systems and extend its application to suspensions of particles with corrugated surfaces and interstitial

solvent. We retain a simple geometrical shape for the particles and account specifically for the solvent associated with the particles. We calculate the birefringence of the rodshaped To-

bacco Mosaic Virus (TMV) particle and of DNA and find excellent agreement between our numerical results and experimental values from the literature.

INTRODUCTION

The theory of birefringence of partially aligned particles in suspension is closely related to the theory of dielectrics which was first developed in the beginning of the 19th century (Landauer, 1978). A general theory of the dielectric constant of mixed systems was published in 1912 by O. Wiener, who obtained expressions for the birefringence of lamellar sheets and suspensions of parallel cylinders. The birefringence of partially aligned ellipsoids in dilute solution under shear flow was examined by Peterlin and Stuart (1939). The birefringence of haemoglobin crystals, measured by Perutz (1953), lead to an article on the birefringence of ellipsoidal particles at arbitrary concentration published by Bragg and Pippard (1953), who pointed out the close relationship between their work and that of Wiener. E. W. Taylor and co-workers (Taylor and Cramer, 1963; Cassim and Taylor, 1965; Cassim et al., 1968) reported a series of measurements on the flow birefringence of protein solutions that seemed to disagree with Wiener's theory. They formulated a new theory that abandoned the assumption of simple geometrical shapes for macromolecules and described instead their dielectric properties by a necklace of induced dipoles. More recent measurements of the birefringence of mitotic spindles (Sato et al., 1975) and of tropomyosin crystals (Ruiz and Oldenbourg, 1988), however, supported the applicability of the original theory.

We propose to reconcile the necklace model with Wiener's theory by accounting specifically for the effect of solvent that is inside the macromolecular structure. Wiener's theory is often cited, but his work was published in a journal which is not readily available and was written in old style German. Therefore, we summarize his impor-

tant results on the dielectric properties of heterogeneous systems. We consider the electric field distribution in polarized suspensions of rotational ellipsoids leading to an exact expression of the dielectric constant for spherical, planar, and rodshaped particles, special cases of the mixture formula for ellipsoids proposed by Bragg and Pippard (1953) on grounds of a less rigorous derivation. We then introduce the concept of corrugated particle surfaces and interstitial solvent. We show that increasing surface corrugation and interstitial solvent amounts decreases the form anisotropy of the particles. We demonstrate the successful application of this concept with model calculations of the birefringence of Tobacco Mosaic Virus (TMV) and DNA and compare these with experimental results in the literature. We conclude by suggesting that birefringence measurements can be used to estimate the amount of solvent associated with fibrous proteins.

THEORY

We are concerned with the average refractive index of a transparent body composed of an isotropic solvent with suspended particles that are small, compared with the wavelength of light. Accordingly, we consider the electric polarization of the body in the quasistatic limit and set the square of the refractive index equal to the dielectric constant of the mixture ($n^2 = \epsilon$, Maxwell relation). C. J. F. Böttcher (1973) suggested a simple formula for the average dielectric constant ϵ of a mixture of nonpolar compounds:

$$\epsilon = \sum_i f_i \epsilon_i. \quad (1)$$

Rudolf Oldenbourg's present address is Marine Biological Laboratory Woods Hole, MA 02543.

ϵ_i is the dielectric constant of the i th component in the pure state. f_i represents the volume fraction of the i th component: $f_i = (N_i)m/(N_i)p$, where $(N_i)m$ is the number of molecules of the i th component in 1 cm^3 of the mixture and $(N_i)p$ the number of molecules in 1 cm^3 of the pure compound. While Eq. 1 predicts remarkably well the measured average dielectric constant of mixed systems (Böttcher, 1973), it fails to account for the anisotropy of the dielectric constant of partially oriented macromolecular systems.

O. Wiener (1912) has developed a general theory for the distribution of the electric field and the dielectric displacement in a heterogeneous system. Suppose that a uniform, external field polarizes the components of a mixture. O. Wiener showed that a simple relationship exists between the average field $\bar{\mathbf{E}}$ in the heterogeneous dielectric body and the average fields $\bar{\mathbf{E}}_i$ in the various components i of the mixture:

$$V\bar{\mathbf{E}} = \sum_i V_i \bar{\mathbf{E}}_i \quad (2)$$

with

$$V_i \bar{\mathbf{E}}_i = \int_{V_i} \bar{\mathbf{E}} \, dv.$$

V_i is the volume of component i and the sum is taken over all components enclosed in the volume V of the mixed body. The same relationship applies for the dielectric displacement $\bar{\mathbf{D}} = \epsilon \bar{\mathbf{E}}$ with ϵ the mean dielectric constant of the mixture:

$$V\epsilon \bar{\mathbf{E}} = \sum_i V_i \epsilon_i \bar{\mathbf{E}}_i \quad (3)$$

ϵ_i is the dielectric constant of the pure compound i . In the appendix we summarize Wiener's derivation of the relationships of Eq. 2 and 3, which are completely general and apply to any heterogeneous mixture. However, to define ϵ in terms of the ϵ_i of the various components, the structure of the mixture has to be specified in more detail. With our final system of oriented, rod-like macromolecules in mind we will consider a suspension of parallel circular cylinders with liquid-like translational order. In a liquid-like arrangement, the surrounding of each rod has the same cylindrical symmetry as the rod itself, if the positions of the neighboring particles are averaged over all possible configurations. As particles cannot overlap, each rod with dielectric constant ϵ_2 is surrounded by a shell of solvent with ϵ_1 . Under these assumptions, the average field $\bar{\mathbf{E}}_2$ inside one particle is related to the average field $\bar{\mathbf{E}}_1$ in the solvent surrounding the particle by:

$$\bar{\mathbf{E}}_2 = \frac{\bar{\mathbf{E}}_1}{1 + \left\{ \frac{\epsilon_2 - \epsilon_1}{\epsilon_1} \right\} A_x} \quad (4)$$

The parameter A_x is the depolarizing factor that depends on the orientation of the rods with respect to the external field. For a field parallel to the rod axes, A_1 is zero and the fields inside the rod and in the solvent are the same. If, however, the long axis is perpendicular to the external field, the depolarizing factor A_\perp is $1/2$, and the field inside the rod is reduced ($\epsilon_2 > \epsilon_1$) or enhanced ($\epsilon_2 < \epsilon_1$). We show in the appendix that Eq. 4 is exact for systems with cylindrical, spherical or planar symmetry and we discuss its applicability to systems with ellipsoidal symmetry. In the case of planar symmetry for fields oriented in the plane (perpendicular to the normal) $A_\perp = 0$, and parallel to the normal $A_1 = 1$; for spherical symmetry, A_x is isotropic and equal to $1/3$.

From Eqs. 2, 3, and 4 the following expression for the dielectric constant ϵ_x of a suspension of parallel cylinders, of parallel sheets or of spheres is obtained:

$$\epsilon_x = \epsilon_1 + \frac{f(\epsilon_2 - \epsilon_1)}{1 + (1 - f) \left(\frac{\epsilon_2 - \epsilon_1}{\epsilon_1} \right) A_x} \quad (5)$$

f is the volume fraction of the particles in the suspension.

We note that Eq. 5 was derived without reference to molecular polarizabilities or local electric fields. Bragg and Pippard (1953) obtained the same relationship (Eq. 5) starting with the excess polarizability of ellipsoids suspended in a dielectric medium. The random array of ellipsoids was polarized by an external electric field. The field acting on one ellipsoid was figured from the external field plus the average field originating from the polarization of the surrounding particles. Bragg and Pippard's expression for the dielectric constant of a random array of ellipsoids is identical to Eq. 5, which was derived using the average field and dielectric displacement inside and around the particles. Our derivation demonstrates that Eq. 5 is correct for all volume fractions, as long as the surroundings of the particles have the same symmetry as the particles themselves. As Bragg and Pippard pointed out, Eq. 5 also applies extremely well in a cubic array of spheres, even when the packing is quite close.

The anisotropy of the dielectric constant of a random array of parallel rods arises from the anisotropy of the depolarizing coefficient A_x . At high particle concentration (f close to 1) the effect of the depolarizing coefficient is reduced by the factor $(1 - f)$ in the denominator. In physical terms, the internal field inside a particle becomes more isotropic at increasing particle concentration, because a high depolarizing factor is counterbalanced by a high field in the solvent surrounding the particles. Therefore, we expect the form birefringence per unit concentration to drop at large particle concentrations.

The anisotropy of the suspension is also affected by the intrinsic anisotropy of the particle material. As the particles are free to rotate around their symmetry axis, one

observes a cylindrical average of the dielectric tensor of the material. Therefore, in case the particles possess an intrinsic anisotropy, ϵ_2 has to be replaced by ϵ_{21} and ϵ_{22} , representing the diagonal elements of the cylindrically averaged dielectric tensor of the particles.

Macromolecules and molecular aggregates are usually not shaped like smooth homogeneous bodies, but have corrugated surfaces and incorporate pockets of solvent in their structure. We will show that both departures from the ideal geometrical shape decrease the anisotropy of the dielectric constant of oriented macromolecular suspensions.

According to Eq. 3 every component i of a mixture contributes to the overall dielectric displacement with the dielectric constant ϵ_i of the pure material times the average electric field \bar{E}_i inside it. \bar{E}_i depends on the environment around the component. If, for example, spherical solvent droplets are incorporated into a rod-shaped macromolecule, the average field in the droplets is generally different from the average field in the solvent surrounding the particle. More specific, when the external field is parallel to the rod axis, the field in the surrounding solvent is equal to the field inside the rod. If a rod contains droplets of solvent the field inside the rod is no longer homogeneous. Solvent pockets with $\epsilon_1 < \epsilon_2$ and the depolarizing factor of a sphere attract the field lines and reduce the average field in the material with dielectric constant ϵ_2 . Therefore, the dielectric displacement $\bar{E}_2 \times \epsilon_2$ of the rod material is reduced. The net result is a lower dielectric constant ϵ_1 of the suspension, if bulk solvent is transferred as spherical droplets into the rod structure. However, if the external field is perpendicular to the rod axis, the dielectric constant ϵ_\perp increases when solvent is incorporated as droplets into the rod. Therefore, for a given amount of material with dielectric constant ϵ_2 , arranged in parallel rods and suspended in solvent, the anisotropy of the dielectric constant of the suspension, as defined by $\Delta\epsilon = \epsilon_1 - \epsilon_\perp$, decreases when solvent penetrates into the rods. However, the mean dielectric constant $\langle\epsilon\rangle = (\epsilon_1 + 2\epsilon_\perp)/3$ remains almost unaffected by the solvent transfer. With the same arguments one can show that corrugated particle surfaces also reduce $\Delta\epsilon$ without affecting $\langle\epsilon\rangle$.

The prominent effect of corrugated surfaces and interstitial solvent is to reduce the difference in the dielectric constant of the solvent and the material inside the smooth particle surface. For rod-like particles, any shape anisotropy of solvent enclosures is cylindrically averaged by the rotational freedom of the particles. Therefore, the average dielectric constant of the material inside the smooth particle surface can be estimated with Eq. 1, if the volume fraction f_s of solvent associated with the macromolecule is known. In the following calculations of the birefringence of DNA and TMV we estimated f_s from structural data

obtained with x-ray diffraction experiments and published in the literature.

So far we have only considered suspensions of perfectly parallel rods with a birefringence $\Delta n_{\text{sat}} = \sqrt{\epsilon_1} - \sqrt{\epsilon_\perp}$. If the alignment is not perfect, the birefringence is reduced and given by

$$\Delta n = \Delta n_{\text{sat}} \times S, \quad (6)$$

with

$$S = \int_0^\pi f(\theta) \times \frac{1}{2} (3 \cos^2 \theta - 1) \times 2\pi \sin \theta d\theta. \quad (7)$$

S is the orientational order parameter of the distribution function $f(\theta)$, with θ the angle between the rod axis and the symmetry axis of the alignment. For oriented macromolecular solutions, S is usually derived from a theoretical model describing the alignment process (Peterlin and Stuart, 1939). Recently, we were able to measure the orientational distribution in liquid crystalline TMV suspensions with x-ray diffraction experiments (Oldenbourg et al., 1988).

In the next section we present model calculations for the birefringence of oriented solutions of DNA and TMV. Both particles are rodshaped and contain substantial amounts of solvent inside their cylindrical surface. By comparing our numerical results with measured values of the birefringence and the refractive index increment of these systems, we obtained values for the optical anisotropy of the DNA nucleotide pair and the protein subunit of TMV. Furthermore, we can successfully account for the opposite signs of the intrinsic birefringence of the common TMV particle and the helical aggregate of the TMV A-protein.

Model calculation

DNA

The structure of the DNA double helix is often loosely compared with a stack of coins, each coin 0.34-nm thick and ~ 2 nm diam. The coins stand for the pairs of nucleotides that owe their flat shape to the bases stacked in the center of the helix. The bases are highly anisotropic ring structures that are responsible for the negative birefringence of DNA.

We define the surface of DNA as a circular cylinder with 1 nm radius, which is the outer radius of the phosphate groups of the two DNA backbones (all structural data refer to B-DNA; see e.g., Bloomfield et al., 1974). Thus the major and minor grooves of DNA are located within the cylindrical surface. We estimate the volume V_{np} of one mol of nucleotide pairs from the partial specific volume of DNA (0.50 cm³/g) and the molecular weight of one nucleotide pair (653 g/mol): $V_{\text{np}} = v_{\text{DNA}} \times$

$MW_{np} = 327 \text{ cm}^3/\text{mol}$. The volume of 1 mol of cylinder elements, each 0.34 nm-thick and 1 nm radius, is 643 cm^3 . Accordingly, just half the cylinder volume is occupied by the nucleotides, the other half is taken up by solvent, which is located in the grooves. If we divide the solvent volume (316 cm^3) by the molar volume of water (18 cm^3), the most abundant solvent molecule, we obtain ~ 18 water molecules per nucleotide pair. This number is very close to the 19 water molecules per pair that are estimated to fit in the major and minor grooves of B-DNA (Saenger, 1984). Hence, the volume fraction f_s of solvent in the DNA molecule is taken as 0.49 and the average dielectric constant ϵ_{DNA} is estimated using Eq. (1):

$$\epsilon_{DNA} = (1 - f_s)\epsilon_{np} + f_s\epsilon_1. \quad (8)$$

ϵ_1 and ϵ_{np} are the dielectric constants of the solvent and the nucleotide pairs, respectively. ϵ_{np} is expected to be highly anisotropic, therefore we introduce $\epsilon_{np\parallel}$ and $\epsilon_{np\perp}$ for fields oriented parallel and perpendicular to the helix axis. $\epsilon_{np\parallel}$ and $\epsilon_{np\perp}$ are the adjustable parameters. We write:

$$\begin{aligned} \epsilon_{DNA\parallel} &= (1 - f_s)\epsilon_{np\parallel} + f_s\epsilon_1, \\ \epsilon_{DNA\perp} &= (1 - f_s)\epsilon_{np\perp} + f_s\epsilon_1. \end{aligned}$$

The dielectric constant of a suspension of parallel oriented DNA molecules is:

$$\epsilon_x = \epsilon_1 + \frac{f_{DNA}(\epsilon_{DNAx} - \epsilon_1)}{1 + (1 - f_{DNA}) \left\{ \frac{\epsilon_{DNAx} - \epsilon_1}{\epsilon_1} \right\} A_x}, \quad (9)$$

with $A_x = 0$ or $1/2$ depending on the field orientation. The calculation of the volume fraction f_{DNA} of DNA cylinders in the suspension has to include the volume of the water in the grooves, which was attributed to the DNA molecule. Therefore, we write:

$$f_{DNA} = \frac{c \times v_{DNA}}{(1 - f_s)},$$

with c the mass concentration of DNA in the suspension and v_{DNA} its partial specific volume.

The specific birefringence of a fully oriented DNA solution is determined by:

$$\frac{\Delta n_{sat}}{c} = \frac{\sqrt{\epsilon_{\parallel}} - \sqrt{\epsilon_{\perp}}}{c}, \quad (10)$$

and the refractive index increment in dilute solution is

$$\frac{dn}{dc} = \frac{\frac{\sqrt{\epsilon_{\parallel}} + 2\sqrt{\epsilon_{\perp}}}{3} - \sqrt{\epsilon_1}}{c}. \quad (11)$$

Both quantities are known experimentally and suffice to determine $\epsilon_{np\parallel}$ and $\epsilon_{np\perp}$.

N. Stellwagen (1981) measured the birefringence of

dilute suspensions ($c \approx 10 \mu\text{g}/\text{cm}^3$) of well defined DNA fragments oriented close to saturation by transient electric fields. Extrapolation to infinite field strength yielded the specific birefringence $\Delta n_{sat}/c = -6.6 \times 10^{-2} \text{ cm}^3/\text{g}$, which was independent of the molecular weight of DNA. Jolly and Eisenberg (1976) measured the refractive index increment $dn/dc = 0.175 \text{ cm}^3/\text{g}$ of dilute DNA solutions. Both measurements used laser light with a wavelength of 633 nm. Using the solvent refractive index $n_1 = 1.334$ (water), we adjusted numerically the dielectric constants $\epsilon_{np\parallel}$ and $\epsilon_{np\perp}$ of the nucleotide pairs until the values calculated with Eqs. 10 and 11 were equal to the measured values. We obtained:

$$\begin{aligned} n_{np\parallel} &= \sqrt{\epsilon_{np\parallel}} = 1.575, \\ n_{np\perp} &= \sqrt{\epsilon_{np\perp}} = 1.737. \end{aligned}$$

Seeds and Wilkins (1950) have measured a birefringence of -0.11 in an oriented DNA fiber containing ~ 30 vol percent of water. Maret and Fillion have measured similar birefringence values with oriented films of DNA (Maret and Weill, 1983). In closely packed fibers and films, the grooves of adjacent DNA molecules interdigitate and the form anisotropy of the molecule is drastically reduced. If we assume no form anisotropy, we can estimate the refractive index of a DNA fiber using Eq. 1 and the above result of $\epsilon_{np\parallel}$ and $\epsilon_{np\perp}$. This leads to $n_{fiber\parallel} = 1.507$, $n_{fiber\perp} = 1.627$ and $\Delta n_{fiber} = n_{fiber\parallel} - n_{fiber\perp} = -0.12$, in good agreement with experiment.

TMV

The calculation of the birefringence of TMV and the helical aggregate of the TMV A-protein proceeds along the same lines as for DNA. For TMV and the helical aggregate the smooth particle surface is defined as a circular cylinder of radius 9 nm (structural data are taken from Namba and Stubbs, 1986; and Mandelkow et al., 1981). Inside the cylinder, identical protein subunits of molecular weight 17,500 form a helix of pitch 2.3 nm with $16\frac{1}{2}$ subunits per turn. Solvent associated with each particle is contained in a central hole (radius 2 nm), in a helical groove on the outside and in pockets inside the protein shell. The common strain of TMV has a single strand of RNA that follows the basic helix between the protein subunits at a radius of 4 nm. Three nucleotides are bound to each protein subunit. The model calculation proceeds in two steps. First, we derive an expression for the optical polarizability of the helical aggregate. Then we add the polarizability of the RNA, using specific structural data to account for the position of the nucleotides in the TMV particle.

The anisotropic structure of the protein subunit suggested the assignment of two dielectric constants, $\epsilon_{ps\parallel}$ and $\epsilon_{ps\perp}$ for fields oriented either parallel or perpendicular to

the long axis of the subunit. $\epsilon_{ps\parallel}$ and $\epsilon_{ps\perp}$ constitute the adjustable parameters in the problem. In the protein shell of the particle the subunits are arranged with their long axis pointing radially, so that for a field parallel to the helix axis all subunits are polarized along their short axis. If we account for a volume fraction f_s of solvent (ϵ_1) inside the shell, the dielectric constant $\epsilon_{sh\parallel}$ of the shell parallel to the particle axis is calculated with Eq. 1:

$$\epsilon_{sh\parallel} = (1 - f_s)\epsilon_{ps\perp} + f_s\epsilon_1. \quad (12)$$

For a field perpendicular to the shell, the cylindrical averaging process orients half the subunits perpendicular to the field and half the subunits parallel to the field. Hence:

$$\epsilon_{sh\perp} = (1 - f_s) \frac{\epsilon_{ps\parallel} + \epsilon_{ps\perp}}{2} + f_s\epsilon_1. \quad (13)$$

We estimated the volume fraction f_s of solvent between radius 2 and 9 nm as follows: The volume of the protein subunits V_{ps} , per mole of helical turn, is given by the partial specific volume v_{HA} of the helical aggregate ($v_{HA} = 0.735 \text{ cm}^3/\text{g}$, Jaenicke and Lauffer, 1969), the molecular weight of one subunit and the number of subunits per turn:

$$V_{ps} = v_{HA} \times 17,500 \times 16^{1/3} = 2.10 \times 10^5 \text{ cm}^3.$$

The volume of the straight cylindrical shell, per mole of helical turn, is:

$$V_{cs} = \pi(r_o^2 - r_i^2)l \times N_A = 3.35 \times 10^5 \text{ cm}^3,$$

with r_o and r_i the outer and inner radius of the shell (9 and 2 nm, respectively), $l = 2.3 \text{ nm}$ the helical pitch and N_A Avogadro's number. The difference of the two volumes is attributed to the solvent in the structure, which amounts to a volume fraction $f_s = 0.37$ or 425 water molecules per subunit. Most of the solvent is located in the groove on the outside of the protein shell, the rest is found inside the protein structure. (High resolution fiber diffraction experiments of TMV have located ~ 30 ordered water molecules and ~ 50 disordered water molecules per protein subunit, not counting the solvent in the groove; Stubbs, 1988).

The central hole in the Helical Aggregate and in TMV has the same cylindrical symmetry as the protein shell. The hole is filled with solvent, leading to the following expression for the dielectric constant ϵ_{HA} of the complete Helical Aggregate:

$$\epsilon_{HAx} = \epsilon_{shx} + \frac{f_h(\epsilon_1 - \epsilon_{shx})}{1 + (1 - f_h) \left(\frac{\epsilon_1 - \epsilon_{shx}}{\epsilon_{shx}} \right) A_x}, \quad (14)$$

where x stands for parallel or perpendicular and A_x for the depolarizing coefficients of a long cylinder ($A_{\parallel} = 0$,

$A_{\perp} = 1/2$). f_h is the volume fraction of the central hole with respect to the full cylinder ($f_h = 0.05$).

The dielectric constant of a suspension of parallel Helical Aggregates is obtained by the final formula:

$$\epsilon_x = \epsilon_1 + \frac{f_{HA}(\epsilon_{HAx} - \epsilon_1)}{1 + (1 - f_{HA}) \left(\frac{\epsilon_{HAx} - \epsilon_1}{\epsilon_1} \right) A_x}, \quad (15)$$

with A_x again 0 or $1/2$. The volume fraction f_{HA} of the helical aggregate in suspension is derived from the mass concentration c of protein, the partial specific volume v_{HA} of the helical aggregate and the volume fractions f_s and f_h of solvent associated with the helix:

$$f_{HA} = \frac{c \times v_{HA}}{(1 - f_s)(1 - f_h)}.$$

Before we compare calculated numbers with reported experimental results we will derive the corresponding expressions for the complete TMV particle. To this end, we add the polarizabilities of the RNA nucleotides to the dielectric constant of the protein shell. The polarizabilities of the nucleotides is highly anisotropic, therefore it is necessary to account for the orientations of the bases of the nucleotides in the shell. Because all data are cylindrically averaged, only the angles of the bases with respect to the helix axis need to be known. Each subunit has three nucleotides with the base angles 90° , 50° , and 70° , which are the angles between the normal of the base planes and the helix axis (we are grateful to Gerald Stubbs for letting us have the atomic coordinates of the nucleotides, from which the above angles were derived; see also Stubbs and Stauffacher, 1981; Namba and Stubbs, 1986).

We assume that RNA nucleotides have dielectric constants $\epsilon_{n\parallel}$ and $\epsilon_{n\perp}$ that are equal to the dielectric constants of nucleotide pairs in DNA (see preceding section). For a single nucleotide, parallel and perpendicular refer to the normal of the base plane. The flat shape of the bases suggest to use the depolarizing coefficient of a flat oblate when the nucleotides are added to the protein structure. Therefore, $\epsilon_{n\parallel}$ is associated with a depolarizing factor of 1 and $\epsilon_{n\perp}$ with a depolarizing factor of 0.

For an electric field parallel to the TMV rod, the protein subunits are polarized perpendicular to their long axes. The dielectric constants of the three nucleotides add with their projections on the particle axis. This leads to the following expression for the dielectric constant $\epsilon_{cyl\parallel}$ of the TMV cylinder combining the protein subunits and the nucleotides:

$$\epsilon_{cyl\parallel} = \epsilon_{ps\perp} + \frac{f_n(\epsilon_{n\parallel} - \epsilon_{ps\perp})}{1 + (1 - f_n) \left(\frac{\epsilon_{n\parallel} - \epsilon_{ps\perp}}{\epsilon_{ps\perp}} \right)} \times \sum_{i=1}^3 \cos^2 \gamma_i + f_n(\epsilon_{n\perp} - \epsilon_{ps\perp}) \times \sum_{i=1}^3 \sin^2 \gamma_i. \quad (16)$$

f_n is the volume fraction of a single nucleotide in the protein subunit:

$$f_n = \frac{v_{\text{DNA}} \times MW_n}{v_{\text{DNA}} \times MW_n + v_{\text{HA}} \times MW_{\text{ps}}} = 0.013.$$

MW_n is the molecular weight of a single nucleotide (327) and MW_{ps} the molecular weight of a protein subunit (17,500).

For a field perpendicular to the TMV rod, the cylindrical averaging procedure orients half the nucleotide bases with their normals perpendicular to the field direction. The other half of the bases are tilted by an angle $90^\circ - \gamma_i$ away from the field direction. Hence:

$$\epsilon_{\text{cyl},\perp} = \epsilon_{\text{ps}} + \frac{f_n(\epsilon_{\text{n}} - \epsilon_{\text{ps}})}{1 + (1 - f_n)\left(\frac{\epsilon_{\text{n}} - \epsilon_{\text{ps}}}{\epsilon_{\text{ps}}}\right)} \times \frac{1}{2} \sum_{i=1}^3 \sin^2 \gamma_i + f_n(\epsilon_{\text{n},\perp} - \epsilon_{\text{ps}}) \times \frac{1}{2} \left(3 + \sum_{i=1}^3 \cos^2 \gamma_i\right). \quad (17)$$

To obtain the dielectric constants of the TMV shell with interstitial solvent, $\epsilon_{\text{cyl},\parallel}$ and $\epsilon_{\text{cyl},\perp}$ replace $\epsilon_{\text{ps},\perp}$ and ϵ_{ps} in Eqs. 12 and 13. The results are carried over to Eq. 14 to get the dielectric constants $\epsilon_{\text{TMV},\parallel}$ and $\epsilon_{\text{TMV},\perp}$ of the complete TMV particle.

The dielectric constant of a suspension of parallel TMV rods is then obtained from:

$$\epsilon_x = \epsilon_1 + \frac{f_{\text{TMV}}(\epsilon_{\text{TMV},x} - \epsilon_1)}{1 + (1 - f_{\text{TMV}})\left(\frac{\epsilon_{\text{TMV},x} - \epsilon_1}{\epsilon_1}\right)A_x}, \quad (18)$$

with $A_{\parallel} = 0$ and $A_{\perp} = 1/2$. The volume fraction f_{TMV} of TMV in suspension is derived from the mass concentration c of TMV, its partial specific volume v_{TMV} (0.730 cm³/g, Jaenicke and Lauffer, 1969) and the volume fractions f_s and f_h of the solvent associated with the particle:

$$f_{\text{TMV}} = \frac{c \times v_{\text{TMV}}}{(1 - f_s)(1 - f_h)}.$$

The specific birefringence $\Delta n_{\text{sat}}/c$ and the refractive index increment dn/dc of TMV suspensions were calculated using Eqs. 10 and 11. The protein refractive indices $n_{\text{ps},\parallel}$ and $n_{\text{ps},\perp}$ were varied until the calculated values were closest to the measured value of dn/dc ($dn/dc = 0.190$ cm³/g; Taylor and Cramer, 1963) and to the set of measured birefringence values, which are listed in Table 1 with their respective references. A solvent refractive index of 1.335 was used in the calculations, if not indicated otherwise. Note that most formulas in the text show dielectric constants, whereas all values in the table are given as refractive index or birefringence values. In

the following we comment on the results listed in Table 1.

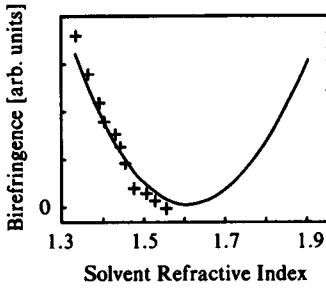
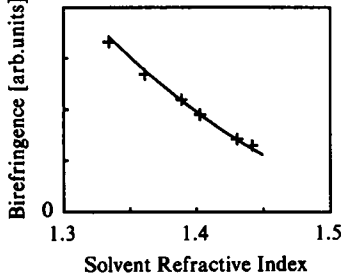
Helical aggregate. The average protein refractive index was found to be 1.59. The refractive index $n_{\text{ps},\parallel}$ parallel to the subunit's long axis is slightly higher than $n_{\text{ps},\perp}$. Contributions to the positive anisotropy of the subunit come from four core α -helices with orientations almost parallel to the long axis of the subunit (Namba and Stubbs, 1986). In a recent article on the birefringence of tropomyosin crystals we have shown experimental evidence that the intrinsic anisotropy of the α -helix is positive ($\Delta n_{\alpha} = 0.011$; Ruiz and Oldenbourg, 1988). Other parts of the amino acid chain, such as aromatic side groups, might also contribute to the positive anisotropy of the protein subunit. The positive anisotropy of the subunit refractive index results in a negative birefringence of the protein helix, because the subunits have their long axes oriented perpendicular to the helix axis. The dry gel of the helical aggregate has indeed a negative birefringence, which was measured by Franklin (1955). The wet gel, however, has a positive birefringence (Franklin, 1955), because the positive form birefringence of the rod becomes dominant at smaller particle concentrations. The protein concentrations in gels of the helical aggregate were assumed to be roughly equal to the concentrations in TMV gels. Comments on the concentration and particle order in the wet and dry gels are summarized below for TMV and do also apply for the Helical Aggregate.

TMV. In the TMV particle, the negative birefringence of the protein helix is overridden by the positive contributions of the nucleotides, resulting in a positive intrinsic birefringence of TMV. Independent support for a positive intrinsic birefringence comes from the observation that TMV orients parallel to a magnetic field (Fraden et al., 1985). Parallel orientation to the field indicates, that TMV has a positive diamagnetic anisotropy. The optical anisotropy is likely to have the same sign, because the anisotropies of the dielectric as well as the diamagnetic susceptibilities originate both from the anisotropic mobility of the electrons in the material.

The intrinsic birefringence of TMV is only weakly positive ($n_{\text{cyl},\parallel} - n_{\text{cyl},\perp} = 1 \times 10^{-4}$). The positive birefringence of oriented TMV solutions arises almost entirely from the form birefringence of the particles. Therefore, one observes an increasing specific birefringence of oriented TMV solutions with decreasing particle concentration.

The largest specific birefringence was observed in dilute TMV suspensions, when a high, transient electric field was applied to induce almost complete orientational order (O'Konski et al., 1959). Extrapolation to infinite

TABLE 1 Birefringences of oriented solutions of TMV and helical aggregates at different particle concentrations c and solvent refractive indices

Sample	$c \left[\frac{g}{cm^3} \right]$	$\frac{\Delta n_{\text{calc}}}{c} \left[\frac{cm^3}{g} \right]$ calculated	$\frac{\Delta n_{\text{meas}}}{c} \left[\frac{cm^3}{g} \right]$ measured	Reference
Helical aggregate	$n_{\text{par}} = 1.591, n_{\text{perp}} = 1.588$			
Wet gel	0.6	0.005	$0.01 > \Delta n$ $\Delta n > 0$	Franklin, 1955
Dry gel	1.1	$-1 \cdot 10^{-5}$	$\Delta n < 0$	Franklin, 1955
TMV	$n_{\text{cyl}} = 1.5929, n_{\text{cyl}\perp} = 1.5928$			
Transient electric birefringence	$4.9 \cdot 10^{-5}$	0.0243	0.0210	O'Konski et al., 1959
Nematic	0.15	0.0200	0.0194	Oldenbourg et al., 1988
Wet gel	0.59	0.007	0.010	Bernal and Fankuchen, 1941
Dry gel	1.08	0.001	0.003	Bernal and Fankuchen, 1941
Flow birefringence				 Lauffer, 1938
Flow birefringence				 Taylor and Cramer, 1963

Specific birefringence values were calculated with the refractive indices n_{par} and n_{perp} of the protein subunit using the model described in the text. Measured values of the specific birefringence were taken from the listed references. The flow birefringences measured by Lauffer were given in arbitrary units. Our calculated values were scaled by a single prefactor to the measured ones. The specific birefringence measured by Taylor and Cramer is $\sim 20\%$ smaller than the value calculated by us and measured with other methods. Therefore, the calculated birefringence curve in the table is multiplied by 0.8 to account for this difference. The refractive indices n_{cyl} and $n_{\text{cyl}\perp}$ refer to the cylindrical average of the refractive index of the protein with RNA nucleotides in the TMV particle.

field strength yielded the listed value for the specific birefringence, which is somewhat smaller than the calculated one.

At higher TMV concentrations, a nematic phase of parallel rods forms spontaneously. The orientational order in magnetically aligned, nematic TMV was measured by us with x-ray diffraction experiments (Oldenbourg et al., 1988).

The particle order in gels of the helical aggregate and of TMV was assumed to be perfectly parallel, with an orientational order parameter $S = 1$. The protein concen-

tration in the wet and dry gels were inferred from the hexagonal lattice constant a measured by x-ray diffraction (wet gel $a = 20.5$ nm; dry gel $a = 15.2$ nm; Bernal and Fankuchen, 1941). The concentration was calculated assuming perfect hexagonal order in the plane perpendicular to the particle axes. The measured lattice constant of 15.2 nm in the dry gel is smaller than the diameter of the particles; therefore, in the dry gel, the protein shells of adjacent particles must interdigitate. It is assumed, however, that the central holes of the particles remain intact. The dry gel still contains $\sim 20\%$ solvent, one third of it is

located in the central holes. For the birefringence calculation of the dry gels, the cylindrical solvent holes were assumed to be embedded in a continuous matrix of protein with the rest of the solvent dispersed evenly in the matrix. The solvents in the dry and wet gels contained an elevated concentration of salt and possibly other organic contaminations. Therefore, the refractive indices of the solvents in the wet and dry gels were probably higher than the refractive index of water. As a rough estimate, we assumed in the calculation a solvent refractive index of 1.35 for the wet gel and of 1.38 for the dry gel.

The flow experiments measured the birefringence of dilute TMV solutions with solvents of various refractive indices. The orientational order induced by the shear flow was not complete and therefore depended on the rate of shear and the solvent viscosities. Lauffer (1938) measured the birefringence of TMV suspensions flowing through a capillary at constant pressure difference, thus inducing the same orientational order in each sample. Taylor and Cramer (1963) measured the induced birefringence in a Rao apparatus and obtained the orientational factor from the measured extinction angle. The calculated birefringence curves are in good agreement with the decrease of the measured flow birefringence with increasing solvent refractive index.

CONCLUSION

We demonstrated that Wiener's theory can be applied successfully to predict the birefringence of oriented suspensions of macromolecules. Our model calculation reflects correctly the measured decrease of the specific birefringence with increasing particle concentrations. In addition, the model accounts for the well known decrease of the birefringence when the solvent refractive index approaches the average refractive index of the protein material. The agreement between experimental and theoretical values was achieved by treating the solvent inside the cylindrical surface of the particles as part of the macromolecules. We showed that the specific birefringence decreases with increasing solvent amounts associated with the macromolecules. Therefore, the observed birefringence of fibrous proteins can be used to estimate the amount of interstitial solvent in the fiber. Thus, birefringence is not only a sensitive indicator of structural anisotropy; it also reveals other important structural information.

APPENDIX

For the derivation of Eqs. 2 and 3, O. Wiener considered the electric field and the dielectric displacement on the surface of a body that is

polarized by an external electric field. He recognized that the mean dielectric constant of a mixed body must be equal to the dielectric constant of a homogeneous body that has the same electric field and dielectric displacement on its surface as the mixed body. Naturally, the two dielectrics, the mixed body, and its homogeneous replacement, have the same boundaries and are polarized by the same external electric field. If the field and the displacement (or charge distribution) on the surface is the same, the field everywhere outside the two bodies must be the same, and hence, the average dielectric constant of the two bodies must be the same. Wiener introduced a small transition region close to the body surface where the field variations of the homogeneous body are smoother than the variations of the field of the heterogeneous body. Fig. 1 is taken from Wiener's original publication and it shows the body surface k and further out the surface g of uniformity beyond which the field of the homogeneous and the heterogeneous body are equal. In the region between k and g the field of the mixed body varies on a smaller scale than that of the homogeneous body. However, we will show that the transition region is usually extremely small compared with the body volume and its effect on the calculation of the mean dielectric constant can be neglected.

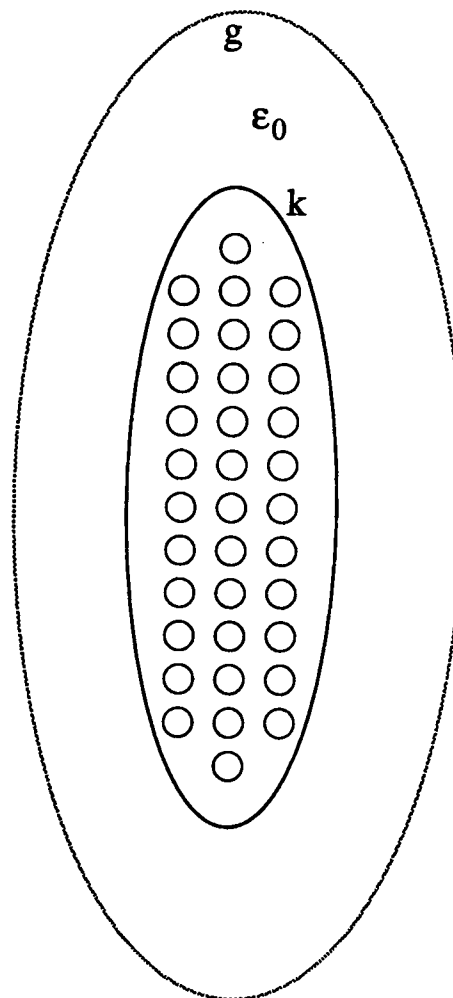


FIGURE 1 Schematic representation of a heterogeneous body with surface k and surface g of uniformity (Wiener, 1912).

Wiener first derived two vector theorems relating volume integrals of a vector \mathbf{A} to surface integrals of the same vector.

The first theorem is related to Stoke's theorem:

If $\nabla \times \mathbf{A} = 0$ within the volume V ,

then
$$\int_V \mathbf{A} \, dv = \frac{1}{2} \int_S \mathbf{A}_t \times \mathbf{x} \, df.$$

S is the surface surrounding the volume V , \mathbf{A}_t is the lateral projection of \mathbf{A} on S and \mathbf{x} is the vector from the origin to the surface element df . \mathbf{A}_t is defined as the cross product of the vector \mathbf{A} and the unit vector \mathbf{e}_n , which is normal to the surface element df . Thus, \mathbf{A}_t is equal in magnitude to the tangential projection of \mathbf{A} but is oriented perpendicular to it.

The second theorem is related to Gauss' theorem:

If $\nabla \cdot \mathbf{A} = 0$ within the volume V ,

then
$$\int_V \mathbf{A} \, dv = \int_S \mathbf{A}_n \times \mathbf{x} \, df.$$

A_n is the magnitude of the projection of \mathbf{A} onto the normal of the surface element df .

We now return to our dielectric problem and first consider the electric field and dielectric displacement at an interface between two components. It is well known that the normal projection \mathbf{D}_n of the dielectric displacement and the tangential or lateral projection \mathbf{E}_t of the electric field is steady by crossing a dielectric interface. Therefore:

$$\mathbf{D}_{ni} = \epsilon_i \mathbf{E}_{ni} = -\epsilon_{i+1} \mathbf{E}_{n(i+1)} = -\mathbf{D}_{n(i+1)}, \quad (\text{A1})$$

$$\mathbf{E}_{ti} = -\mathbf{E}_{t(i+1)}. \quad (\text{A2})$$

i and $(i + 1)$ denote the indices of two adjacent components. The minus signs in Eqs. A1 and A2 have to be included because the normal to the interface of a component points from the interior of the component outwards.

The vector theorems are used to relate the average field $\bar{\mathbf{E}}_i$ and dielectric displacement $\bar{\mathbf{D}}_i$ of component i of the mixed body to their lateral and normal projections at the interface.

$$V_i \times \bar{\mathbf{E}}_i = \int_{V_i} \mathbf{E} \, dv = \int_{S_i} \mathbf{E}_t \times \mathbf{x} \, df, \quad (\text{A3})$$

$$V_i \times \bar{\mathbf{D}}_i = \int_{V_i} \mathbf{D} \, dv = \int_{S_i} \mathbf{D}_n \times \mathbf{x} \, df, \quad (\text{A4})$$

with

$$\mathbf{D} = \epsilon_i \mathbf{E}.$$

V_i is the volume of component i and ϵ_i is its dielectric constant. We form the sum over all interfaces between all components i including the body surface k , which is the boundary, when looking from outside the body. Each interface appears twice in the sum, once with each of the two components touching at the interface. Because of the relationships Eqs. A1 and A2, the sum over all interfaces must be zero:

$$\int_{S_k} \mathbf{E}_t \times \mathbf{x} \, df + \sum_i \int_{S_i} \mathbf{E}_t \times \mathbf{x} \, df = 0, \quad (\text{A5})$$

$$\int_{S_k} \mathbf{D}_n \times \mathbf{x} \, df + \sum_i \int_{S_i} \mathbf{D}_n \times \mathbf{x} \, df = 0. \quad (\text{A6})$$

We add to Eqs. A5 and A6 the corresponding surface integrals for the

outer surface g of uniformity:

$$\int_{S_k} \mathbf{E}_t \times \mathbf{x} \, df + \int_{S_g} \mathbf{E}_t \times \mathbf{x} \, df + \sum_i \int_{S_i} \mathbf{E}_t \times \mathbf{x} \, df = \int_{S_g} \mathbf{E}_t \times \mathbf{x} \, df, \quad (\text{A7})$$

$$\int_{S_k} \mathbf{D}_n \times \mathbf{x} \, df + \int_{S_g} \mathbf{D}_n \times \mathbf{x} \, df + \sum_i \int_{S_i} \mathbf{D}_n \times \mathbf{x} \, df = \int_{S_g} \mathbf{D}_n \times \mathbf{x} \, df. \quad (\text{A8})$$

The two terms in front of the sum signs are equal to the volume average of the field and the displacement in the region between the surface of the mixed body and the surface g of uniformity. We denote this region with index 0 and rewrite Eqs. A7 and A8 with all surface integrals on the l.h.s. replaced by the volume averages of the fields and displacements (Eqs. A3 and A4):

$$V_0 \bar{\mathbf{E}}_0 + \sum_i V_i \bar{\mathbf{E}}_i = \int_{S_g} \mathbf{E}_t \times \mathbf{x} \, df, \quad (\text{A9})$$

$$V_0 \bar{\mathbf{D}}_0 + \sum_i V_i \bar{\mathbf{D}}_i = \int_{S_g} \mathbf{D}_n \times \mathbf{x} \, df. \quad (\text{A10})$$

The same derivation applies to the homogeneous body with dielectric constant ϵ which replaces the mixed body without altering the field and the displacement at the surface g . Therefore:

$$V_0 \bar{\mathbf{E}}'_0 + V \bar{\mathbf{E}} = \int_{S_g} \mathbf{E}_t \times \mathbf{x} \, df, \quad (\text{A11})$$

$$V_0 \bar{\mathbf{D}}'_0 + V \bar{\mathbf{D}} = \int_{S_g} \mathbf{D}_n \times \mathbf{x} \, df. \quad (\text{A12})$$

The primes account for the possibility that the field and the displacement in the transition region close to the body surface might be different for the homogeneous and the heterogeneous body. We equate the left sides of Eqs. A9 and A11 and correspondingly Eqs. A10 and A12, rearrange the terms and obtain:

$$\bar{\mathbf{E}} = (\bar{\mathbf{E}}'_0 - \bar{\mathbf{E}}_0) V_0/V + \sum_i f_i \bar{\mathbf{E}}_i, \quad (\text{A13})$$

$$\bar{\mathbf{D}} = (\bar{\mathbf{D}}'_0 - \bar{\mathbf{D}}_0) V_0/V + \sum_i f_i \bar{\mathbf{D}}_i. \quad (\text{A14})$$

f_i is the volume fraction V_i/V of component i in the mixed body. With Eq. A13 A14 Wiener has found a very suggestive relationship between the average field (displacement) inside the homogeneous body and the average field (displacement) inside the various components of the heterogeneous mixture.

The question remains, what is the magnitude of the term involving the region next to the surface of the two bodies? It seems reasonable to assume that the extension d_0 of the volume V_0 perpendicular to the body surface is of the same order as the average size l_i of the components of the mixture. The volume ratio V_0/V is then equal to $1/l$ with l the typical size of the mixed body. Hence, for macromolecular solutions with $l_i = 1 \dots 100$ nm and $l \sim 1$ cm, V_0/V is a very small quantity ($10^{-7} \dots 10^{-5}$). Furthermore, the differences $(\bar{\mathbf{D}}'_0 - \bar{\mathbf{E}}_0)$ and $(\bar{\mathbf{D}}'_0 - \bar{\mathbf{D}}_0)$ ought to be very small themselves and arguments might be found to show that the differences are close to zero, if not zero altogether. The field variation in the lateral direction near the surface k of the heterogeneous body is on the same scale as the size of the constituent components. If the field is averaged over lateral directions much larger than the size of the components, the average field near the body surface k must be close to

the average field near the surface g where it is equal to the field of the homogeneous body. Thus, the differences $(\bar{\mathbf{E}}_0 - \bar{\mathbf{E}}_g)$ and $(\bar{\mathbf{D}}_0 - \bar{\mathbf{D}}_g)$ should indeed be close to zero. Therefore, it seems justified to neglect the terms involving the transition region and we write:

$$\bar{\mathbf{E}} = \sum_i f_i \bar{\mathbf{E}}_i, \quad (\text{A15})$$

$$\bar{\mathbf{D}} = \sum_i f_i \bar{\mathbf{D}}_i, \quad (\text{A16a})$$

$$\text{or} \quad \epsilon \bar{\mathbf{E}} = \sum_i f_i \epsilon_i \bar{\mathbf{E}}_i. \quad (\text{A16b})$$

Eqs. A15 and A16a, b correspond to Eqs. 2 and 3 in the main text and they apply to any heterogeneous dielectric body, regardless of the shape of its components and their arrangement in the body.

Finally, we consider the special case of an infinitely long rod with dielectric constant ϵ_2 covered with a concentric cylindrical shell with dielectric constant ϵ_1 . The rod with shell is placed in an infinite medium with yet another dielectric constant and is polarized by a uniform external electric field. The mixed system has complete cylindrical symmetry and its polarization in a homogeneous external field can be solved exactly. For any field direction, the field \mathbf{E}_2 in the central rod is homogeneous. If the external field is parallel or perpendicular to the rod axis, the average field $\bar{\mathbf{E}}_1 = \int_{V_{\text{shell}}} \mathbf{E} \, dv$ in the shell is colinear with \mathbf{E}_2 and the following relationship between $\bar{\mathbf{E}}_1$ and \mathbf{E}_2 holds:

$$\mathbf{E}_2 = \frac{\bar{\mathbf{E}}_1}{1 + \left[\frac{\epsilon_2 - \epsilon_1}{\epsilon_1} \right] A_x}. \quad (\text{A17})$$

A_x is the depolarizing factor which depends on the orientation of the external field with respect to the cylinder axis ($A_1 = 0$ and $A_\perp = 1/2$). Eq. A17 is also correct for systems with planar symmetry ($A_1 = 1$ and $A_\perp = 0$) and spherical symmetry, in which case A_x is isotropic and equal to $1/3$. Note that Eq. A17 is independent of the thickness of the shell. Furthermore, Eq. A17 is independent of what comes beyond the shell, as long as the outside space possesses the same symmetry as the particles. If the outer surface of the shell moves to infinity, Eq. A17 corresponds to the well-known result for a single particle embedded in an infinite dielectric medium. $\bar{\mathbf{E}}_1$ is then equal to the uniform external field polarizing the medium.

If the central particle is a rotational ellipsoid with a confocal shell, we found that Eq. A17 is not exact, but represents a first approximation.

An interesting case left to analyze is the ellipsoid of revolution with a concentric shell that has the same axial ratio as the inner surface. At the moment we do not know if Eq. A17 is exact for this case.

We gratefully acknowledge helpful discussions and support by D. L. D. Caspar and R. B. Meyer.

The work was supported in part by Public Health Service grant 5R01CA15468 from the National Cancer Institute awarded to D. L. D. Caspar.

Received for publication 12 December 1988 and in final form 13 March 1989.

REFERENCES

- Bernal, J. D., and I. Fankuchen. 1941. X-ray and crystallographic studies of plant virus preparations. *J. Gen. Physiol.* 25:111-165.
- Bloomfield, V. A., D. M. Crothers, and I. Tinoco. 1974. Physical chemistry of nucleic acids. Harper and Row Publishers, New York.
- Böttcher, C. J. F. 1973. Theory of Electric Polarization, 2nd ed. Vol. 1. Elsevier North-Holland Biomedical Press, Amsterdam.
- Bragg, W. L., and A. B. Pippard. 1953. The form birefringence of macromolecules. *Acta Cryst.* 6:865-867.
- Cassim, J. Y., and E. W. Taylor. 1965. Intrinsic birefringence of poly-g-benzyl-L-glutamate, a helical polypeptide, and the theory of birefringence. *Biophys. J.* 5:531-552.
- Cassim, J. Y., P. S. Tobias, and E. W. Taylor. 1968. Birefringence of muscle proteins and the problem of structural birefringence. *Biochim. Biophys. Acta.* 168:463-471.
- Fraden, S., A. J. Hurd, R. B. Meyer, M. Cahoon, and D. L. D. Caspar. 1985. Magnetic-field-induced alignment and instabilities in ordered colloids of Tobacco Mosaic Virus. *J. Physique* 46: C3:85-113.
- Franklin, R. E. 1955. Structural resemblance between Schramm's repolymerized A-protein and Tobacco Mosaic Virus. *Biochim. Biophys. Acta.* 18:313-314.
- Jaenicke, R., and M. A. Lauffer. 1969. Polymerization-depolymerization of Tobacco Mosaic Virus protein. XII. Further studies on the role of water. *Biochemistry.* 8:3083-3092.
- Jolly, D., and H. Eisenberg. 1976. Photon correlation spectroscopy, total intensity light scattering with laser radiation and hydrodynamic studies of a well fractionated DNA Sample. *Biopolymers.* 15:61-95.
- Landauer, R. 1978. Electrical conductivity in inhomogeneous media. (With an excellent review on the historical development of the dielectric theory of inhomogeneous media). *AIP Conf. Proc.* 40:2-45.
- Lauffer, M. 1938. Optical properties of solutions of Tobacco Mosaic Virus protein. *J. Phys. Chem.* 42:935-944.
- Mandelkow, E., G. Stubbs, and S. Warren. 1981. Structures of helical aggregates of Tobacco Mosaic Virus protein. *J. Mol. Biol.* 152:375-386.
- Maret, G., and G. Weill. 1983. Magnetic birefringence study of the electrostatic and intrinsic persistence length of DNA. *Biopolymers.* 22:2727-2744.
- Namba, K., and G. Stubbs. 1986. Structure of Tobacco Mosaic Virus at 3.6 Å resolution: implications for assembly. *Science (Wash. DC).* 231:1401-1406.
- O'Konski, C. T., K. Yoshioka, and W. H. Orttung. 1959. Electric properties of macromolecules. IV. Determination of electric and optical parameters from saturation of electric birefringence in solutions. *J. Phys. Chem.* 63:1558-1565.
- Oldenbourg, R., X. Wen, R. B. Meyer, and D. L. D. Caspar. 1988. Orientational distribution function in nematic Tobacco Mosaic Virus liquid crystals measured by x-ray diffraction. *Phys. Rev. Lett.* 61:1851-1854.
- Perutz, M. F. 1953. Polarization dichroism, form birefringence and molecular orientation in crystalline haemoglobins. *Acta. Crystallogr.* 6:859-864.
- Peterlin, A., and H. A. Stuart. 1939. Zur theorie der strömungsdoppelbrechung von kolloiden und großen molekülen in lösung. *Z. Phys. Chem.* 112:1-19.
- Ruiz, T., and R. Oldenbourg. 1988. Birefringence of tropomyosin crystals. *Biophys. J.* 54:17-24.
- Saenger, W. 1984. Principles of Nucleic Acid Structure. Springer-Verlag New York, Inc., NY.
- Sato, H., G. W. Ellis, and S. Inoué. 1975. Microtubular origin of mitotic spindle form birefringence. Demonstration of the applicability of Wiener's equation. *J. Cell Biol.* 67:501-517.

-
- Seeds, W. E., M. H. F. Wilkins. 1950. Ultra-violet microspectrographic studies of nucleoproteins and crystals of biological interest. *Faraday Discuss. Chem. Soc.* 9:417-423.
- Stellwagen, N. C. 1981. Electric birefringence of restriction enzyme fragments of DNA: optical factor and electric polarizability as a function of molecular weight. *Biopolymers*. 20:399-434.
- Stubbs, G., and C. Stauffacher. 1981. Structure of the RNA in Tobacco Mosaic Virus. *J. Mol. Biol.* 152:387-396.
- Taylor, E. W., and W. Cramer. 1963. Birefringence of protein solutions and biological systems. I and II. *Biophys. J.* 3:127-154.
- Tsvetkov, V. N. 1963. The optical effect of the shape of rigid polymer chains in solutions. II. Experimental. *Polym. Sci. USSR*. 4:1456-1464.
- Wiener, O. 1912. Die Theorie des mischkörpers für das feld der stationären strömung. erste abhandlung. Die mittelwertsätze für kraft, polarisation und energie. *Abhandl. Math. Phys. Klas. Königl. Sächs. Gesellsch. Wissensch.* 23:509-604.